Journal of the Korean Electrochemcal Society
Vol. 2, No. 1, 1999, 38-45

Lithium intercalation into a plasma-enhanced-chemical-vapour-deposited carbon film electrode

Su-Il Pyun†

Department of Materials Science and Engineering, Korea Advanced Institute of Science and Technology, Taejon 305-701, Korea

(Received November 9, 1998 : Accepted January 15, 1999)

Abstract

Electrochemical lithium intercalation into a PECVD (plasma enhanced chemical vapour deposited) carbon film electrode was investigated in 1 M $LiPF_6$-EC (ethylene carbonate) and DEC (diethyl carbonate) solution during lithium intercalation and deintercalation, by using cyclic voltammetry supplemented with ac-impedance spectroscopy. The size of the graphitic crystallite in the a- and c-axis directions obtained from the carbon film electrode was much smaller than those of the graphite one, indicating less-developed crystalline structure with hydrogen bonded to carbon, from the results of AES (Auger electron spectroscopy), powder XRD (X-ray diffraction) method, and FTIR(Fourier transform infra-red) spectroscopy. It was shown from the cyclic voltammograms and ac-impedance spectra of carbon film electrode that a threshold overpotential was needed to overcome an activation barrier to entrance of lithium into the carbon film electrode, such as the poor crystalline structure of the carbon film electrode showing disordered carbon and the presence of residual hydrogen in its structure. The experimental results were discussed in terms of the effect of host carbon structure on the lithium intercalation capability.

Key words : Carbon film electrode, Cyclic voltammetry, Lithium rechargeable battery, Plasma enhanced chemical vapour deposition method

1. Introduction

Pyrolytic carbon[1-3] from hydrocarbon source was manufactured by using plasma enhanced chemical vapour deposition (PECVD) method, since the radio frequency (RF) excited plasma[4] exposes the substrate to positive ions and to electrons alternatively and thus prevents any net charge accumulation on insulating deposits. In this case, it has been the subject of controversy whether the hydrogen atom connected to carbon atom affects the lithium intercalation capability* beneficially or detrimentally.

In so far as carbonaceous materials showing desirable electrode behaviour is concerned, pyrolytic carbon, obtained by chemical vapour deposition of hydrocarbon, has been studied to examine the charge-discharge behaviour in relation to the microscopic structure[5,6] since, in the structure of pyrolytic carbon, there exists disordered carbon[7,8] which is the carbon that is not associated with planar graphite-like layer. Reportedly, pyrolytic carbon electrode shows good reversibility, and the battery comprising the pyrolytic carbon has a long cycle life and endures deep discharge.

In relation to the pyrolytic carbon where the characteristics of disordered carbon appear, what has to be noticed is to understand the mechanism of capacity loss in disordered carbons which exhibit a considerable irreversible capacity loss that leads to deterioration in the reversible cell capacity.[9] Thus many studies were performed to examine the charge/discharge behaviour and lithium doping sites of negative electrodes, for example, cokes heat-treated at relatively low temperatures near 1000°C.[10] Moreover, the correlation between the layer spacing d_{002} and the capacity for various disordered carbons has been reported by many researchers[8] in order to understand the influence of these structures on the kinetics of the intercalation, considering that carbon materials generally have large variations in their crystal structure.

The intercalation mechanism in disordered carbon has been recently proposed by many researchers, that is, doping/undoping of lithium in the interior of carbon. The lower deintercalation capacity than intercalation capacity was explained by the lithium trapping inside carbon.[11] Under these circumstances, carbons prepared by CVD method were of interest to reveal the capacity loss in disordered carbon in relation with the disorder in carbon host. Furthermore, it is necessary to use the CVD film specimen with the well-defined reaction area in order to quantitatively analyze ac-impedance spectra.

In this respect, the present study aims at exploring the lithium intercalation into the carbon film electrode depending upon the structure of pyrolytic carbon as a host carbon, by using cyclic voltammetry combined with ac-impedance spectroscopy. For this purpose, the structure of pyrolytic carbon was characterized with AES (Auger electron spectroscopy),

*This is sometimes termed capacity

†E-mail : sipyun@sorak.kaist.ac.kr

powder XRD (X-ray diffraction) method, and FTIR (Fourier transform infra-red) spectroscopy. Pyrolytic carbon electrode in the form of film specimen prepared by PECVD (plasma enhanced chemical vapour deposition) method and 1 M $LiPF_6$ in EC (ethylene carbonate) and DEC (diethylene carbonate) were chosen as an intercalation electrode and a non-aqueous electrolyte, respectively.

2. Experimental

Carbon film, ca. 100 nm in thickness, was prepared by using PECVD method onto copper plate with a thickness of 0.09 mm at a temperature of 600°C. The mixture of methane and hydrogen with a C/H ratio of 1/7 was used as a source gas at a total chamber pressure of 45 Pa. Before deposition, the copper plate used as a substrate was cut into sections approximately 1×1 cm in size and then mechanically polished with # 2000 emery paper and successively with alumina powder.

To characterize crystal structure of the carbon film electrode deposited, powder X-ray diffraction collected from the carbon deposit on alumina substrate was carried out according to the method defined by Gakushin (JSPS), using a X-ray diffractometer (Rigaku Geigerflex; Cu K_α, 0.15406 nm, 40 kV, 30 mA). All measurements were made between 10 and 80° in scattering angle with a scan rate of 4° min^{-1}.

FTIR spectrum of the carbon film electrode obtained were measured by a transmission method to investigate the chemical structure of the surface on the carbon film electrode. The interference caused by the multiple reflection of the beam was eliminated by using computer programs. In addition, AES was employed to study the compositional changes in carbon and copper near the carbon-copper interface and the interfacial reaction at the carbon-copper interface. Auger measurements were made by using a cylindrical mirror analyzer with a coaxial electron gun of the Perkin-Elmer PHI 4300 scanning Auger microprobe system. Auger data were taken with a primary electron beam energy of 3 keV and a modulation voltage of 1 V (peak-to-peak). The carbon film electrode was investigated, firstly, in the surface survey mode in the range 50~1500 eV and then Auger electron depth profiling was performed after pre-treatment with an argon sputter gun.

For the electrochemical measurements, a three-electrode cell was employed in a glove box (MECAPLEX GB94) filled with purified argon gas at room temperature. The carbon film electrode was used as working electrode. Both reference and counter electrodes were made of lithium foil (Foote Mineral Co. U.S.A., purity 99.9%). The electrolyte used here was 1 M solution of $LiPF_6$ dissolved in a 50 : 50 vol.% mixture of EC and DEC.

Cyclic voltammograms were obtained from passivated carbon film electrode in 1 M $LiPF_6$-EC/DEC in the potential range of 2.0 $V_{Li/Li+}$ to 10 $mV_{Li/Li+}$ with a scan rate of 1 mVs^{-1}, by using a Potentiostat/Galvanostat (EG&G Model 273) to determine intercalation characteristics of the electrode. The impedance spectra were obtained from passivated carbon film electrode at various applied potentials. The electrochemical impedance measurements were carried out by using frequency response analyzer (Solartron, SI 1255 FRA) in conjunction with potentiostat (Solartron, SI 1286 ECI) in the glove box. Impedance spectra were potentiostatically measured by applying an ac voltage of 10 mV_{RMS} amplitude over the frequency ranging from 10^{-2} to 10^5 Hz. The frequency was scanned from high to low value. The measurements were collected after the electrode attained steady-state relationship between current and potential, that is, after the 10th cycle by avoiding the influence of any irreversible phenomenon occurring during the first cycle.

3. Results and discussion

Fig. 1 demonstrates Auger electron spectrum in the surface survey mode for the carbon film electrode in the kinetic energy range of 50 to 1500 eV. The peak at about 270 eV makes the deposits identified as carbon, since the peak at 270 eV accords well with the energy location of minimum, 271 eV, in the first derivative of C-KLL Auger spectra.[12] The peak pertaining to hydrogen, which is supposed to be contained in the structure of the carbon film electrode due to the incomplete decomposition of source gases, methane and hydrogen, did not appear since the hydrogen peak fell below the Auger electron kinetic energy of 50 eV.

Fig. 2 presents the Auger electron depth profile across carbon film, carbon-copper interface and copper substrate obtained from the carbon film electrode. It was calculated from the depth profile that carbon film was ca. 100 nm in thickness. At the interface of carbon film and copper substrate, copper carbide was formed, leading to enhanced adhesion of carbon film to the copper substrate. As will be shown later in cyclic voltammetry, the carbon film electrode shows stable intercalation and deintercalation currents after passivating film formation without detachment of the carbon deposit,

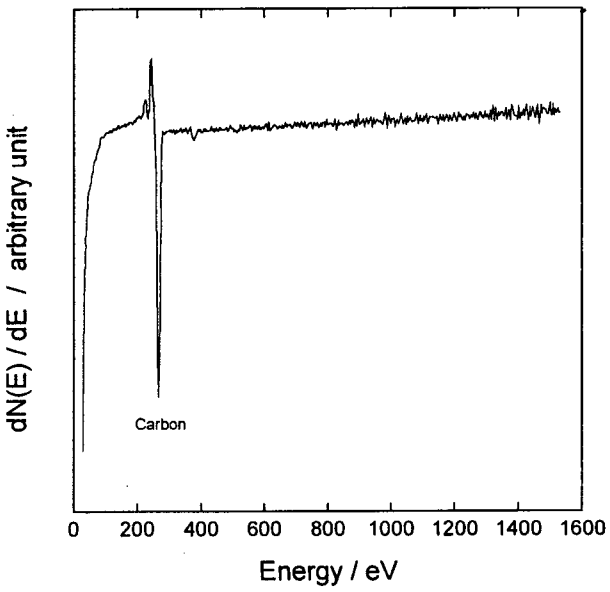

Fig. 1. High resolution Auger spectrum obtained from the surface of carbon film electrode in the energy range of 50 to 1500 eV.

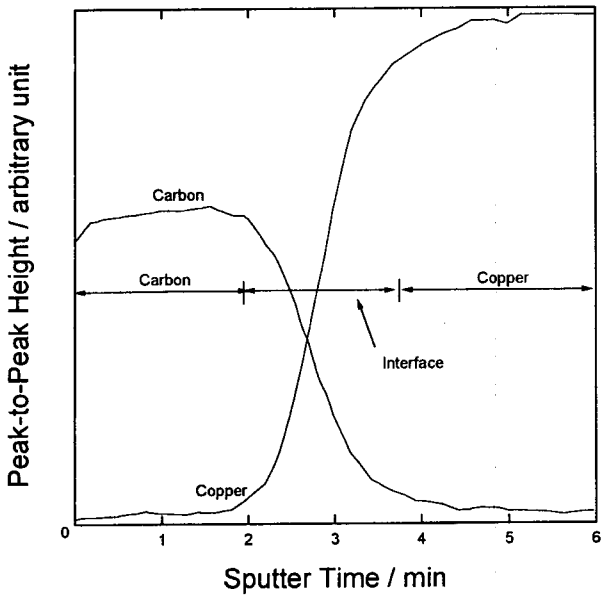

Fig. 2. Auger microprobe depth profile analysis of carbon and copper peaks at the carbon-copper interface of the carbon film electrode on copper substrate.

due to the enhanced adhesion at the interface of carbon and copper substrate.

Fig. 3 exhibits FTIR spectrum of the carbon film electrode obtained by subtracting interference effect. In the range of 2980 to 2850 cm^{-1}, three characteristic peaks marked with closed circles were observed in the aliphatic C-H stretching region.[13] These three kinds of C-H absorption peaks are found in tabulations of the C-H stretching in the region[14,15] which brings about qualitative information on sp^2- and sp^3-coordinated carbons. Thus, it is possible that, in the carbon film electrode, there exist three types of C-H bonds: aromatic sp^2-C and H, aliphatic sp^2-C and H, and sp^3-C and H (deconvolution method).

It is suggested that, from the observation of C-H stretching, substantial amount of hydrogen atoms are linked to the carbon atoms in the carbon film electrode, possibly to the disordered carbon. It is easily supposed that hydrogen in the structure of the carbon film electrode originated from the pyrolysis of methane and hydrogen, arising from the remnant hydrogen in the pyrolysis. The remainder hydrogen effect on the lithium intercalation capability is of great interest in that the hydrogen enhances or hinders the lithium intercalation.

Fig. 4 shows powder XRD pattern for the carbon film electrode prepared by using PECVD method. The broad diffraction peak near 20° indicates that the carbon film electrode in this work has smaller size of graphitic crystallite than the graphite one. That is to say, the dimensions of the crystallite in the a- and c-axis directions, L_a and L_c, determined from the half-width value of the diffraction peak, were 2.06 and 1.01 nm, respectively, according to the Scherrer's equation:

$$L_a = 1.84\lambda/(\beta\cos\theta)$$
$$L_c = 0.89\lambda/(\beta\cos\theta)$$

where λ is the wave length of the X-ray beam (0.154 nm), θ is the Bragg angle, and β is the amount of broadening due to the specimen, usually the half-width value of the diffraction peak. The graphite electrode, in which case sharp (002) Bragg peak appears,[16,17] has larger crystallite size than that of the carbon film electrode in this work, indicating well-developed stacks of parallel layer planes. The diffraction peak near 20° which is located at a lower angle than the diffraction peak of 26.5° in the case of graphite electrode denotes that the interlayer spacing of the carbon film electrode in this work is larger than the graphite one.

In essence, X-ray diffraction analysis shows that the carbon film electrode in this work has values for L_a and L_c in the range of 1 to 2 nm, which indicate that the carbon deposits are composed of an assemblage, which is possibly in spheri-

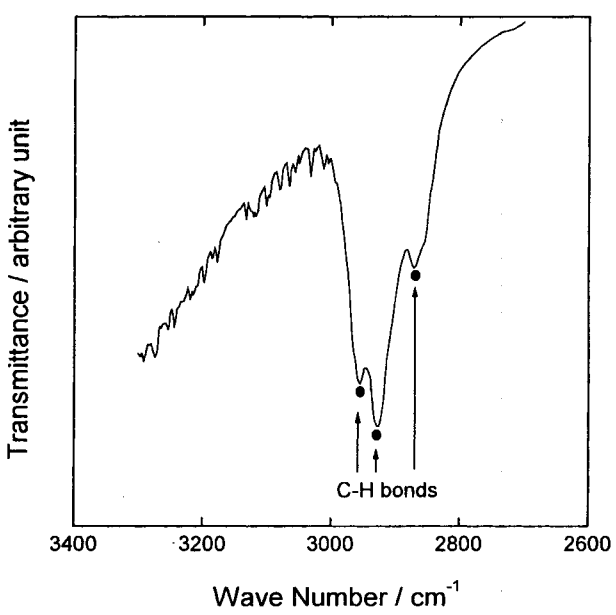

Fig. 3. FTIR spectrum obtained from the carbon film electrode.

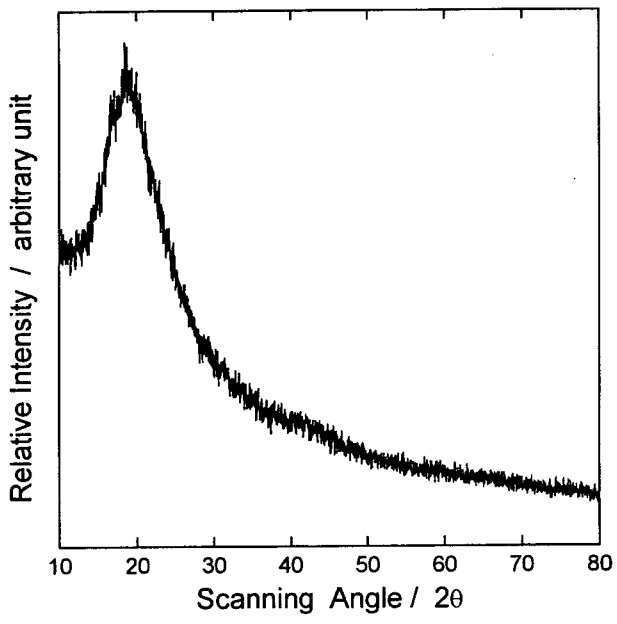

Fig. 4. XRD pattern of the carbon film electrode.

cal shape, of many quasi-graphitic crystallites with the layer dimensions mentioned above. Furthermore, the larger d_{002}-spacing of carbon film electrode compared to that of graphite (0.345 nm) indicates that the layer planes are not in register but are simply parallel with no three-dimensional order.

It is worthwhile to note that this kind of carbon deposit is different from typical turbostratic carbons in that the carbon deposit has larger d_{002}-spacing than the turbostratic carbons. This is attributable to the increased amount of unorganized carbon due to the residual hydrogen in the carbon deposit[18] as evidenced by the three characteristic peaks in FTIR spectrum in the aliphatic C-H stretching region.

From the above structural analyses of XRD and FTIR complemented by the analysis of AES, it is suggested that the deposited material proved to be a poorly crystallized carbon containing substantial amounts of hydrogen. As a matter of fact, it is possible to distinguish certain kinds of carbons by the difference in lithium intercalation capability.[19] In this regard, it is conceivable to closely correlate electrochemical lithium intercalation into the carbon film electrode with the structure of the electrode. It is also noticeable how hydrogen in the structure affects intercalation capability.

Fig. 5 displays cyclic voltammograms obtained from the carbon film electrode in 1 M $LiPF_6$-EC/DEC solution in the scan range of 3 $V_{Li/Li+}$ to 10 $mV_{Li/Li+}$ with a scan rate of 1 mV s^{-1}. The cathodic current at the first intercalation decreased with successive cycling. This irreversible behaviour during the first intercalation indicates the formation of passivating film on the surface of the carbon film electrode caused by salt and solvent reduction.[20] After the first intercalation, cyclic voltammograms showed nearly invariant shapes indicating reversible intercalation and deintercalation of lithium since the passivating film formed on the electrode makes lithium intercalate and deintercalate reversibly.

Broad anodic peak above 2 $V_{Li/Li+}$ was observed in the case of the carbon film electrode, indicating that the lithium intercalation/deintercalation took place in the higher potential region than that of the graphite.[21] In other words, in contrast to the graphite, the anodic current tends to increase with the increase in applied potential without conspicuous anodic peaks. In this sense the increase in the amount of the disordered carbon which is helped by the residual hydrogen is supposed to act as a structural barrier to the lithium deintercalation as well as intercalation, indicating the detrimental effect of the disordered carbon and residual hydrogen on the intercalation behaviour.

Further cyclic voltammetry will show a qualitative measure of structural barrier to lithium intercalation. That is, successive decrease in the lower potential limit in order to increase the overpotential needed to intercalate more amount of lithium, can help to qualitatively estimate the structural barrier to lithium intercalation. Fig. 6 gives successive cyclic voltammograms of the carbon film electrode in the potential range of 1 to 0, -0.1, and -0.2 $V_{Li/Li+}$ in order to disclose the effect of the overpotential on lithium intercalation.

From the cyclic voltammogram during the 11th cycle in the potential range of 1 to 0 $V_{Li/Li+}$, no distinct anodic peak appeared, indicating that only a small amount of lithium is intercalated and it is rarely deintercalated. It was indicated that some amount of lithium ions was trapped in the region of disorganized carbon. With further decreasing negative potential limit by way of -0.1 to -0.2 $V_{Li/Li+}$, anodic peak which is supposed to be attributable to the deintercalation of lithium appeared more unambiguously, indicating more lithium is intercalated with increasing overpotential.

It is not always possible to exclude the effect of lithium deposition on the anodic peak because the anodic peak is shifted to the more positive potential. Nonetheless, the anodic

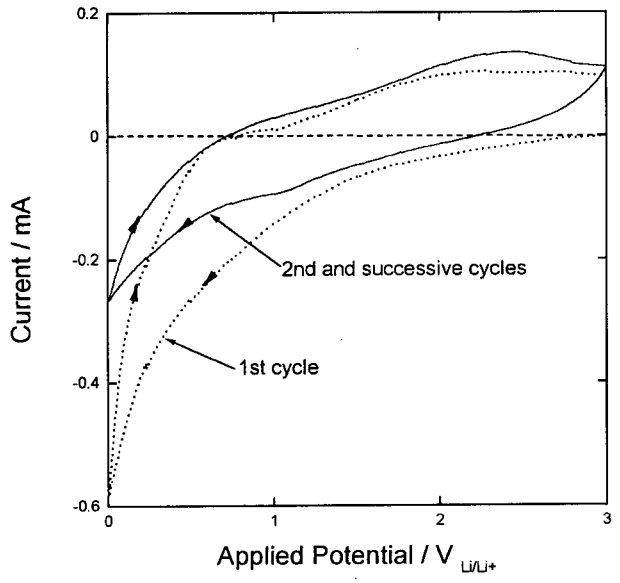

Fig. 5. Cyclic voltammograms obtained from the carbon film electrode in 1 M $LiPF_6$-EC/DEC solution in the potential range of 3 V to 10 $mV_{Li/Li+}$ with a scan rate of 1 mV s^{-1}.

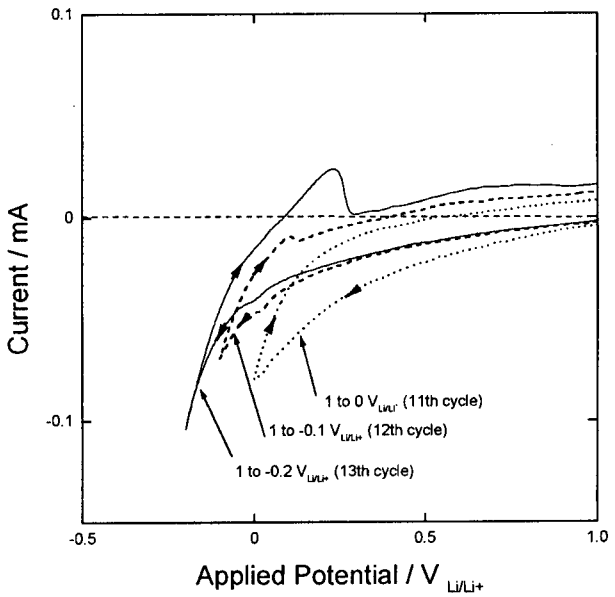

Fig. 6. Successive cyclic voltammograms obtained from the carbon film electrode in 1 M $LiPF_6$-EC/DEC solution after the first intercalation in the potential range of 1 to 0, -0.1 and -0.2 $V_{Li/Li+}$ with a scan rate of 1 mV s^{-1}.

peak is not solely attributed to the lithium deposition but also to the lithium intercalation into the carbon structure, which will be more clear from the extension of the lower limit of applied potential in the more negative direction.

In cyclic voltammograms extended to a negative applied potential, it was reported[22] that lithium deposition and dissolution are likely to occur on the passivating film formed during the first intercalation. In the literature, the anodic peak is associated with the cathodic reaction including lithium deposition followed by intercalation of lithium. It is believed that the effect of lithium deposition is ruled out since the deposited lithium was easily detached from the electrode surface and then dissolved in the electrolyte when potential scan was reversed. This is evidenced by the fact that the anodic peak at about 0.1 $V_{Li/Li+}$ in the cyclic voltammogram of which the negative potential limit was -0.1 $V_{Li/Li+}$ diminished when the negative potential limit was extended to -0.2 $V_{Li/Li+}$ arising from the poor adhesion of lithium deposited on surface film of carbon electrode.

Fig. 7 reveals successive cyclic voltammograms of the carbon film electrode in the potential range of 1 to -0.3, -0.4, and -0.5 $V_{Li/Li+}$. It is observed that the current level during anodic scan was lower than that during cathodic scan until the potential at which the cathodic and anodic branches intersect in the cyclic voltammogram, which was not found in the previous cyclic voltammogram (Fig. 6). This behaviour is anomalous and is not generally expected, because, in metal system, the current level during anodic scan diminishes due to the oxide film formation.

However, it is of great importance to consider the unexpected increase in cathodic current level during reverse scan in cyclic voltammogram which was not considered seriously. This abnormal behaviour in cyclic voltammogram is thought to be attributable to the lithium deposition on the surface of carbon surface. This results from the fast recombination of electron and lithium ion at the interface of carbon electrode and electrolyte because of the high driving force for electron transfer through the electrode. The lithium deposition phenomenon in the cyclic voltammograms can be supported later by the impedance spectra.

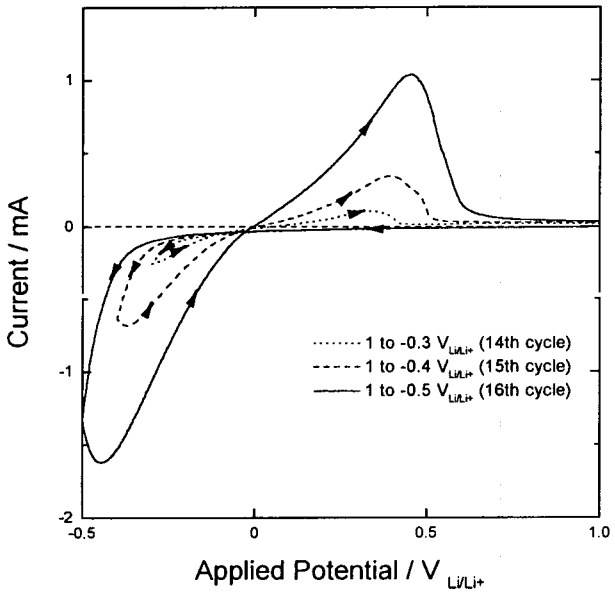

Fig. 7. Successive cyclic voltammogram obtained from the carbon film electrode in 1 M $LiPF_6$-EC/DEC solution after the first intercalation in the potential range of 1 to -0.3, -0.4 and -0.5 $V_{Li/Li+}$ with a scan rate of 1 mV s^{-1}.

One can not exclude the possibility of the unexpected increase in current level during reverse scan in cyclic voltammogram, which was known[23,24] to appear in the same way that lithium is not intercalated, but simply deposited on an inert electrode like platinum electrode during the cathodic scan and then detached from the electrode during the anodic scan. In this regard, it is inferred that the increase in current level during anodic scan in cyclic voltammogram can be accounted for by the fact that some portion of lithium, which is deposited on the carbon film electrode by applying the overpotential higher than threshold overpotential necessary for lithium intercalation, is easily detached during the anodic scan and at the same time lithium deposition proceeds successively to a greater extent despite of reverse scan.

Moreover, in the cyclic voltammograms of the carbon film electrode in the potential range of 1 to -0.3, -0.4, and -0.5 $V_{Li/Li+}$, the anodic peaks appear clearly and show small change in their location, indicating deintercalation of lithium in addition to dissolution of lithium previously deposited. In this sense a threshold overpotential to overcome the activation barrier to lithium intercalation is about -0.3 $V_{Li/Li+}$. Here, the anodic peak in the cyclic voltammograms of the carbon film electrode in the potential range of 1 to -0.1, and -0.2 $V_{Li/Li+}$ is supposed to be mainly caused by lithium deposition.

From cyclic voltammograms of Figs. 6 and 7, it is clear that intercalation into and deintercalation from the carbon film electrode do not result from reciprocal mechanisms,[23] which is the reason why a threshold overpotential is needed to overcome activation barrier to intercalation of lithium. As mentioned earlier, the disordered carbon influenced by the residual hydrogen and small amount of graphitic crystallite as well can contributes to the activation barrier. The threshold overpotential, which makes it possible for the anodic (deintercalation) peak to appear, is important to characterize the intercalation capability of the carbon depending upon the structural disorder.

Fig. 8 demonstrates the Nyquist plots of impedance spectra obtained from the carbon film electrode in 1 M $LiPF_6$-EC/DEC solution at the applied potentials of 1, 0.5, 0.3, 0.2, 0.1, and 0.01 $V_{Li/Li+}$. The size of the mixed loop decreased as the applied potential decreased. This means that the resistance pertaining to the mixed loop decreased with decreasing applied potential. It followed from this result that charge transfer resistance decreased with greater driving force for lithium intercalation since the main contribution to the mixed loop was ascribed to charge transfer reaction.[25]

Based upon the carbon/organic electrolyte interface model similar to the lithium interface model,[26] the impedance spectra of the carbon film electrode is assumed to comprise the mixture of possibly two basic loops corresponding to the migration process in the passivating film on the carbon film

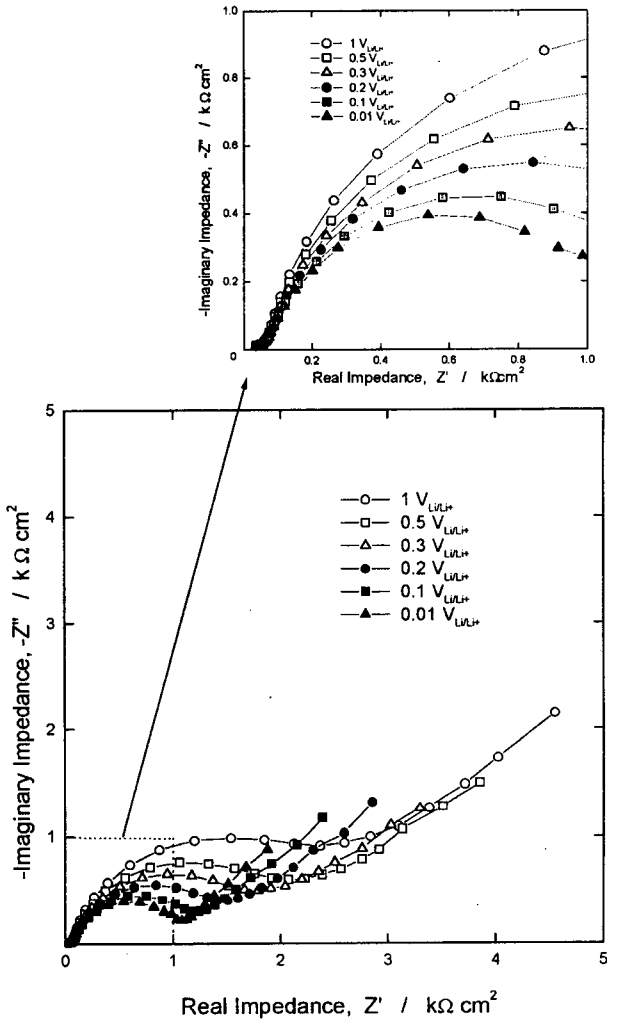

Fig. 8. Impedance spectra in Nyquist presentation obtained from the carbon film electrode in 1 M $LiPF_6$-EC/DEC solution in the frequency range of 5×10^{-2} to 10^5 Hz at the applied potentials of: (○) 1 $V_{Li/Li+}$; (□) 0.5 $V_{Li/Li+}$; (△) 0.3 $V_{Li/Li+}$; (●) 0.2 $V_{Li/Li+}$; (■) 0.1 $V_{Li/Li+}$; (▲) 0.01 $V_{Li/Li+}$.

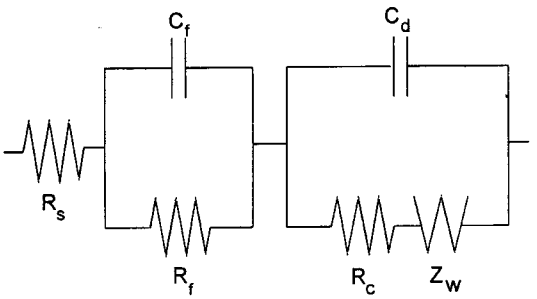

Fig. 9. Equivalent circuit describing the interface between electrolyte and carbon film electrode. R_s: the solution resistance, R_c: the charge-transfer resistance, R_f: the resistance associated with passivating film, Z_w: the Warburg impedance, and C_d anc C_f: the capacities corresponding to R_c and R_f, respectively.

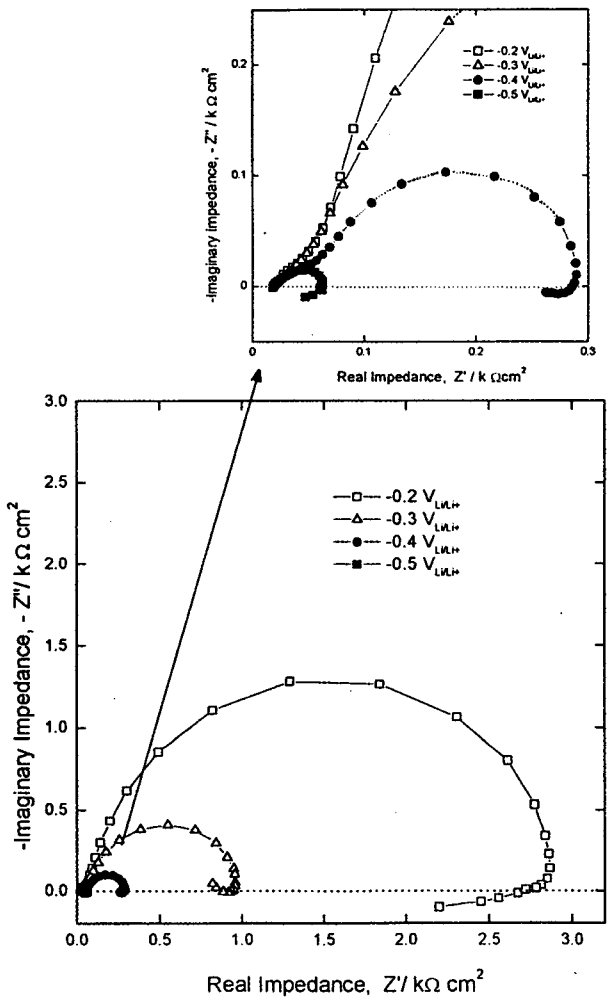

Fig. 10. Impedance spectra in Nyquist presentation obtained from the carbon film electrode in 1 M $LiPF_6$-EC/DEC solution in the frequency range of 5×10^{-2} to 10^5 Hz at the applied potentials of: (□) -0.2 $V_{Li/Li+}$; (△) -0.3 $V_{Li/Li+}$; (●) -0.4 $V_{Li/Li+}$; (■) -0.5 $V_{Li/Li+}$.

electrode (high frequency range) and the charge transfer at the interface between solution and passivating film (medium frequency range), followed by straight line corresponding to the diffusion process of lithium not merely within the passivating layer but also within the carbon by way of passivating layer(low frequency range) under the application of potentials above 0 $V_{Li/Li+}$.

The impedance of the film-covered carbon/electrolyte interface can be modeled by a simple equivalent circuit, as illustrated in Fig. 9. This kind of impedance spectra was analyzed by adopting the equivalent circuit to estimate each element in equivalent circuit, by using fitting method first written by Macdonald *et al.*[27] and then modified in this laboratory.[28]

Fig. 10 presents the Nyquist plots of impedance spectra obtained from the carbon film electrode in 1 M $LiPF_6$-EC/DEC solution at the applied potentials of -0.2, -0.3, -0.4, and -0.5 $V_{Li/Li+}$. The impedance spectra of the carbon film electrodes are composed of the mixture of possibly two basic loops with almost similar relaxation times in the high and middle frequency range, followed by a inductive arc in the low frequency range under the application of potentials below 0 $V_{Li/Li+}$. The resistance pertaining to the mixed loop followed the same trend as the former one in Fig. 8. Besides, the presence of the inductive arc explains the formation of reaction

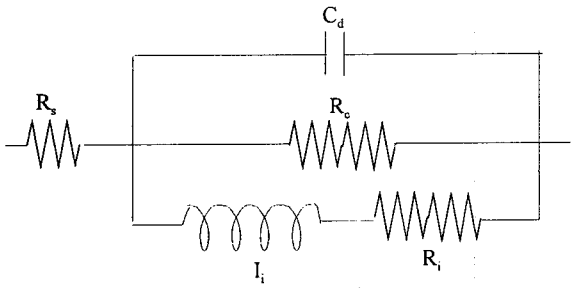

Fig. 11 Equivalent circuit describing the interface between electrolyte and carbon film electrode. R_s: the solution resistance, R_c: the charge-transfer resistance, R_i: the resistance associated with coated lithium metal, I_i: the inductance corresponding to R_i, C_d: the capacity corresponding to R_c.

intermediate[29] on the surface of the carbon film electrode, which is, in the present work, supposed as the lithium metal coated on the carbon surface due to the application of potential below 0 $V_{Li/Li+}$,[30] as mentioned above in analyzing cyclic voltammograms.

This kind of impedance spectra can be modeled by an equivalent circuit, as illustrated in Fig. 11. The impedance spectra in this work could be understood according to the Epelboin model[31] which analyzes the impedance spectra in the presence of reaction intermediate[29] on the surface of the electrode.

Distinction between the two types of impedance spectra with respect to the applied potential is attributed to difference in driving force of lithium transport toward the electrode, *i.e.*, increased driving force for lithium transport toward the electrode under the application of potential below 0 $V_{Li/Li+}$. Hence, in the latter type of impedance spectra, the inductive arc appeared in the low frequency range, explaining that lithium deposition occurs along with lithium intercalation into the electrode. The drastic decrease in charge transfer resistance below -0.2 $V_{Li/Li+}$ explains the commencement of deintercalation peak in cyclic voltammogram, resulting from the enhanced intercalation of lithium at the applied potentials below -0.2 $V_{Li/Li+}$.

4. Conclusions

The lithium intercalation into the carbon film electrode in 1 M $LiPF_6$-EC/DEC solution depending upon the structure of the electrode was investigated by using powder XRD method, FTIR spectroscopy, AES and cyclic voltammetry in conjunction with ac-impedance spectroscopy. The conclusions are drawn as follows:

1. The broad XRD peak of the carbon film electrode, which is shifted to a lower angle than the graphite one, indicates a less-developed crystalline structure than that of graphite. The carbon film electrode also contained substantial amount of hydrogen, as evidenced by the result of FTIR spectroscopy.

2. After the first intercalation, intercalation into and deintercalation from the carbon film electrode do not proceed by reciprocal mechanisms, indicating the detrimental effect of the disordered carbon and residual hydrogen on the intercalation behaviour.

3. From the cyclic voltammogram during the 11th cycle in the potential range of 1 to 0 $V_{Li/Li+}$, it was indicated that some amount of lithium ions was trapped in the region of disorganized carbon. With further decreasing negative potential limit by way of -0.1, -0.2, -0.3, and -0.4 to -0.5 $V_{Li/Li+}$, anodic peak which is supposed to be attributable to the deintercalation of lithium appeared more unambiguously, indicating more lithium is intercalated with increasing overpotential in addition to the lithium deposition on the carbon surface.

4. From the ac-impedance spectra under the application of potentials above 0 $V_{Li/Li+}$, it was shown that the charge transfer resistance decreased as the applied potential was lowered, indicating the rising driving force for lithium intercalation. From the ac-impedance spectra under the application of potentials below 0 $V_{Li/Li+}$, it is indicated that the presence of the inductive arc accounts for the lithium deposition on the carbon surface by the application of potential below 0 $V_{Li/Li+}$.

Acknowledgment

This work was supported in the period of 1995/1997 by the Korea Science and Engineering Foundation through the Center for Interface Science and Engineering of Materials at Korea Advanced Institute of Science and Technology (KAIST). The author is deeply indebted to Mr. S.-W. Kim for his analysis of the experimental data with helpful suggestions.

References

1. L. Holland and S. M Ojha, *Thin Solid Films,* **48**, L21 (1978).
2. B. Dischler and E. Bayer, *J. Appl. Phys.,* **68**, 1237 (1990).
3. L. Holland and S. M Ojha, *Thin Solid Films,* **38**, L17 (1996).
4. M. Shimozuma, G. Tochitani, H. Ohno, H. Tagashira and J. Nakahara, *J. Appl. Phys.,* **66**, 447 (1989).
5. M. Mohri, N. Yanagisawa, Y. Tajima, H. Tanaka, T. Mitate, S. Nakajima, M. Yoshida, Y. Yoshimoto, T. Suzuki and H. Wada, *J. Power Sources,* **26**, 545 (1989).
6. R. Schlesinger, M. Bruns and H.-J. Ache, *J. Electrochem. Soc.,* **144**(1), 6 (1997).
7. R. E. Franklin, *Acta Cryst.,* **3**, 107 (1950).
8. F. A. Heckman, *Rubber Chem. Technol.,* **37**, 1245 (1964).
9. W. Xing, J. S. Xue, A. Gibaud and J. R. Dahn, *J. Electrochem. Soc.,* **143**(11), 3482 (1996).
10. Y. Mori, T. Iriyama, T. Hashimoto, S. Yamazaki, F. Kawakami, H. Shiroki and T. Yamabe, *J. Power Sources,* **56**, 205 (1995).
11. Y. Matsuda, M.Ishikawa, T. Nakamura, M. Morita, S.-I. Tsujioka and T. Kawashima, "The electrochemical society proceedings; Rechargeable lithium and lithium ion (RCT) batteries", S. A. Megahed (Ed.), Vol.28, p.85, The Electrochemical Society, Inc. (1994).
12. L. E. Davis, N. C. MacDonald, P. W. Palmberg, G. E. Riach and R. E. Weber, "Handbook of Auger Electron Spectroscopy", p. 29, Physical Electronics Div., Perkin-Elmer, Eden-Prairie, MN, USA (1976).
13. J. Zawadzki, "Chemistry and Physics of Carbon", P. L. Walker (Ed.), Vol. 21, p. 148, Marcel Dekker, New York, USA (1989).
14. G. Herzberg, "Infrared and Raman Spectra of Polyatomic

Molecules", p. 118, Van Nostrand, Prinston, NJ (1945).
15. F. R. Dollish, W. G. Fateley and F. F. Bentley, "Characteristic Raman Frequencies of organic compounds", p. 248, Wiley, New York, USA (1974).
16. D. B. Fischbach, "Chemistry and Physics of Carbon", P. L. Walker (Ed.), Vol. 7, p. 1, Marcel Dekker, New York, USA (1971).
17. A. Satoh, N. Takami and T. Ohsaki, *Solid State Ionics,* **80**, 291 (1995).
18. J. C. Bokros, "Chemistry and Physics of Carbon", P. L. Walker (Ed.), Vol. 5, p. 1, Marcel Dekker, New York, USA (1966).
19. J. R. Dahn, A. K. Sleigh, H. Shi, J. N. Reimers, Q. Zhong and B. M. Way, *Electrochim. Acta,* **38**, 1179 (1993).
20. Y.-G. Ryu and S.-I. Pyun, *J. Electroanal. Chem.,* **433**, 97 (1997).
21. J. R. Dahn, A. K. Sleigh, H. Shi, B. M. Way, W. J. Weydanz, J. N. Reimers, Q. Zhong and U. von Sacken, "Lithium Batteries: New Materials, Developments, and Perspectives", G. Pistoia (Ed.), p. 1, Elsevier (1994).
22. D. Pletcher, J. F. Rohan and A. G. Ritshie, *Electrochim. Acta,* **39**, 1369 (1994).
23. R. Yazami and D. Gue'rard, *J. Power Sources,* **43-44**, 39 (1993).
24. J. O. Besenhard, *Carbon,* **14**, 111 (1976).
25. N. Takami, A. Satoh, M. Hara and T. Ohsaki, *J. Electrochem. Soc.,* **142**, 371 (1995).
26. M. Gaberscek, J. Jamnik and S. Pejovnik, J. Electrochem. Soc., 140(2), 308 (1993).
27. J. R. Macdonald, W. B. Johnson, "Impedance Spectroscopy", J. R. Macdonald (Ed.), p. 1, Wiley, New York, USA (1987).
28. J.-S. Bae and S.-I. Pyun, *J. Mat. Sci. Lett.,* **13**, 573 (1994).
29. S.-I. Pyun and Y.-G. Ryu, *J. Power Sources,* **62**, 1 (1996).
30. S.-I. Pyun, press in *J. Mat. Sci. Letters* (1999).
31. I. Epelboin, M. Keddam and J. C. Lestrade, *Trans. Faraday Soc.,* **75**, 264 (1973).